Proton transfer vs. oligophosphine formation by P-C/P-H sigma-bond metathesis : decoding the competing Bronsted and Lewis type reactivities of imidazolio-phosphines

Cicac-Hudi, Mario

2020-12-21

Cicac-Hudi , M , Feil , C M , Birchall , N , Nieger , M & Gudat , D 2020 , ' Proton transfer vs. oligophosphine formation by P-C/P-H sigma-bond metathesis : decoding the competing Bronsted and Lewis type reactivities of imidazolio-phosphines ' , Dalton Transactions , vol. 49 , no. 47 , pp. 17401-17413 . https://doi.org/10.1039/d0dt03633a

http://hdl.handle.net/10138/336101
https://doi.org/10.1039/d0dt03633a

unspecified
acceptedVersion

Dalton Transactions

An international journal of inorganic chemistry

Accepted Manuscript

This article can be cited before page numbers have been issued, to do this please use: M. Cicac-Hudi, C. M. Feil, N. Birchall, M. Nieger and D. Gudat, *Dalton Trans.*, 2020, DOI: 10.1039/D0DT03633A.

This is an Accepted Manuscript, which has been through the Royal Society of Chemistry peer review process and has been accepted for publication.

Accepted Manuscripts are published online shortly after acceptance, before technical editing, formatting and proof reading. Using this free service, authors can make their results available to the community, in citable form, before we publish the edited article. We will replace this Accepted Manuscript with the edited and formatted Advance Article as soon as it is available.

You can find more information about Accepted Manuscripts in the Information for Authors.

Please note that technical editing may introduce minor changes to the text and/or graphics, which may alter content. The journal's standard Terms & Conditions and the Ethical guidelines still apply. In no event shall the Royal Society of Chemistry be held responsible for any errors or omissions in this Accepted Manuscript or any consequences arising from the use of any information it contains.

ROYAL SOCIETY OF CHEMISTRY

rsc.li/dalton

View Article Online
DOI: 10.1039/D0DT03633A

ARTICLE

Proton transfer vs. oligophosphine formation by P–C/P–H σ-bond metathesis: decoding the competing Brønsted and Lewis type reactivity of imidazolio-phosphines

Received 00th January 20xx,
Accepted 00th January 20xx

DOI: 10.1039/x0xx00000x

Mario Cicač-Hudi,[a] Christoph M. Feil,[a] Nicholas Birchall,[a] Martin Nieger [b] and Dietrich Gudat*[a]

Studies of the protonation and alkylation of imidazolio-phosphides and deprotonation of imidazolio-phosphines reveal a complex behaviour that can be traced back to an interplay of Brønsted-type proton transfers and Lewis-type P–P bond formation reactions. As a consequence, the expected (de)protonation and (de)alkylation processes compete with reactions producing cyclic or linear oligophosphines. Careful adjustment of the conditions allows selectively address each reaction channel and devise specific syntheses for primary, secondary and tertiary imidazolio-phosphines, imidazolio-alkylphosphides, and cyclic oligophosphines, respectively. Mechanistic studies reveal that the oligophosphines assemble in sequential P–P bond formation steps involving condensation of cationic imidazolio-phosphines via σ-bond metathesis and concomitant elimination of an imidazolium ion. Imidazolio-phosphides catalyse these transformations. Computational model studies suggest that the metathesis proceeds in two stages via an initial nucleophilic substitution under expulsion of a carbene, and a subsequent proton transfer step which generates the imidazolium cation and provides the driving force for the whole transformation. As energy barriers are predicted to be low or even absent, different elementary steps are presumed to form a network of mutually coupled equilibrium processes. Cyclic oligophosphines or their dismutation products are identified as the thermodynamically favoured final products in the reaction network.

Introduction

Construction and breakdown of frameworks of P–P single bonds plays a key role in processes like the transformation of elemental phosphorus into simple molecular phosphorus compounds or metal polyphosphides,[1] both of which have relevance in academia and industry. The structural features and relative stabilities of neutral,[1c,2] anionic,[1c,2,3] and even cationic[4] P_n-frameworks are meanwhile well known, and also the initial stages in the gradual activation of white phosphorus are in principle understood.[1c,d] It is clear that phosphide anions, which can be created by action of nucleophiles or reductants on elemental phosphorus or by deprotonating PH-functionalised phosphines, may act as promoters. However, even if the assembly and disassembly of complex P_n-architectures were occasionally elucidated in some detail,[1,2b] many mechanistic issues remain still in the dark.

We have now found that "imidazolylidene-phosphinidenes" **I-X** (Chart 1)[5] provide a new and unexpected avenue to P–P bond formation reactions. These compounds have since their discovery garnered continuous attention, presumably because the synthesis from an N-heterocyclic carbene (NHC) and a cyclic oligophosphine led to perceive them as Lewis-complexes of elusive phosphinidenes.[6,7] Particular interesting seemed P-functionalized specimens like **I-H**[8,9] and **I-Si**,[10] which offer a route to further derivatives through substituent exchange.[8b,10] Derivatization of a P–H bond was also reported for **II-H**, which can be formally regarded as phosphinidene complexes of CC-saturated imidazoline-2-ylidenes.[11]

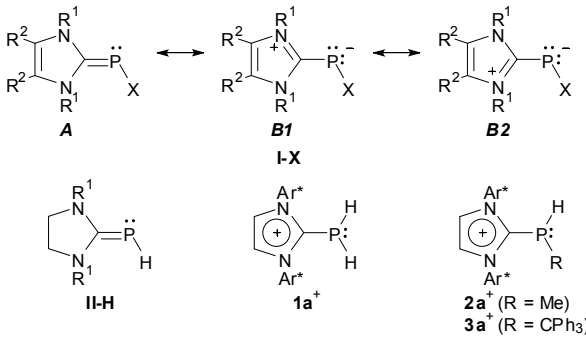

Chart 1: Molecular structures of **I-X** (X = Ph, CF_3, H, $SiMe_3$; R^1 = alkyl, aryl; R^2 = H, Me), **II-H** (R^1 = aryl) and imidazolio-phosphines **1a⁺ - 3a⁺** (Ar* = 2,6-bis(benzhydryl-4-methyl-phenyl).

However, fragmentation of **I-X** under transfer of a phosphinidene to another substrate, which would allow utilize these compounds as a viable entry point into phosphorus(I)

[a] Institute of Inorganic Chemistry, University of Stuttgart, Pfaffenwaldring 55, 70550 Stuttgart, Germany.
[b] Department of Chemistry, University of Helsinki, P.O. Box 55, 00014 University of Helsinki, Finland.

Electronic Supplementary Information (ESI) available: Experimental procedures. Representations of NMR, IR, mas spectra, results of crystallographic and computational studies. CCDC-1992146 to 1992153, 1992155 to 1992158. See DOI: 10.1039/x0xx00000x

chemistry, has to the best of our knowledge not been reported. Whilst a solitary account on P-Ph-transfer from a Zn-complex of **I-Ph**[12] and the sporadic observation of related transformations for acyclic analogues of **I-X**[13] insinuates that these processes are not totally unfeasible, they do not seem to be a preferred reaction channel. This conjecture is rationalised by recalling that the accepted representation of the bonding in **I-X** through superposition of a leading canonical structure ***A*** with large contributions from "ylidic" structures ***B1, B2***,[5,6] which was recently validated by a computational study on **I-H**,[14] results in a P–C bond order between one and two and implies a fairly robust nature of the NHC–PR skeleton. In line with the contribution of the ylidic resonance structures, **I-X** display rather a phosphide-like behaviour that is evidenced in first reports on the protonation or alkylation to cationic species like **1a**$^+$**-3a**$^+$[15] or the ability to bind as ligand to two metal centres or borane units,[15,16] respectively. In order to highlight this reactivity, we will denote compounds **I-X** from now on as "imidazolio-phosphides".

Cations **1a**$^+$**-3a**$^+$ are analogues of tertiary carbenio-phosphines whose positive charge resides mainly on the N-heterocyclic substituent,[17] but their chemical properties remain, in contrast to those of the tertiary congeners, largely unexplored. We reasoned that cationic alkylphosphines like **2a**$^+$ and **3a**$^+$ might react with bases, like other secondary phosphines, under deprotonation to afford rare imidazolio-alkylphosphides,[6b,18] and that the alkylation/deprotonation sequence can offer an evidence-based mechanistic explanation for previously reported[8b] substitution reactions. As we reveal here, a thorough study of the acid/base chemistry of representatives of **I-H** and their protonation and alkylation products allowed us prove these conjectures, but unveiled as well more complex reactivity patterns that are characterized by a rivalry between proton transfer and P–P bond formation processes. The latter proceed under σ-bond metathesis with elimination of imidazolium cations and are to the best of our knowledge the first reactions involving formal "R–P" transfer from un-complexed imidazolio-phosphines.‡ Our investigations show further how each reaction channel can be addressed by adaption of the reaction conditions, and give mechanistic insight into an ostensible phosphinidene transfer process that helps advance the general understanding of this important class of reactions.

Results and Discussion

Protonation and alkylation of primary imidazolio-phosphides.

The pioneering study on imidazolio-phosphide protonation reports on the reaction of a sterically congested derivative with triflic acid (CF_3SO_3H).[15] The choice of reactants was obviously motivated by the desire to stabilize cation **1a**$^+$, which was presumed to be chemically fragile, by extremely bulky N-aryl substituents and a weakly nucleophilic anion. We found now that analogues of **1a**$^+$ are readily accessible upon addition of less shielded or even unprotected imidazolio-phosphides **4b-e** to tetrafluoroboric or aqueous hydroiodic acid (Scheme 1). The resulting salts are isolable in crystalline form and are thermally stable regardless of the degree of steric protection. Their synthesis implies that cations **1**$^+$ tolerate even a nucleophilic counter ion (I^-) and water, and must thus be viewed as chemically quite robust.

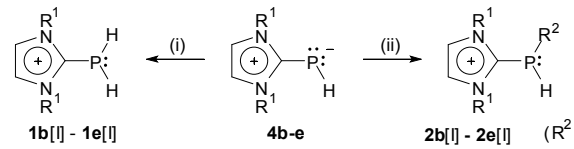

Scheme 1: Synthesis of salts of primary ((**1b-e**)$^+$) and secondary ((**2b-e**)$^+$, (**5b-e**)$^+$) imidazolio-phosphines. Reagents and conditions: (i) 1.5 equivs. of aq. HI or aq. HBF_4, toluene, -78 °C – rt: (ii) 1 equiv. of MeI or $[R^2_3O][BF_4]$, MeCN, rt; R^1 = 2,6-*i*Pr$_2$C$_6$H$_3$ (Dipp, **1b**$^+$ - **5b**$^+$), 2,4,6-Me$_3$C$_6$H$_2$ (Mes, **1c**$^+$ - **5c**$^+$), *i*Pr (**1d**$^+$ - **5d**$^+$), Me (**1e**$^+$ - **5e**$^+$).

Like **4a**,[15] sterically less protected imidazolio-phosphides **4b–e** undergo also alkylation with methyl iodide or Meerwein salts to afford isolable salts of secondary cations (**2b-e**)$^+$ or (**5c–e**)$^+$, respectively (Scheme 1). The selectivity and yield were found to depend on the reaction conditions; the best results were obtained when the imidazolio-phosphide was added to a solution of the electrophile in a polar solvent like acetonitrile.

The isolated salts were characterized by spectroscopic and analytical data and, in several cases, by single-crystal X-ray diffraction studies (Figure 1 and ESI). The crystals contain arrays of well separated anions and cations. The coordination geometry at the phosphorus atoms is pyramidal. There is no evidence for P–H···X hydrogen bonding, but several specimens display weak X···P contacts (2.91 to 3.37 Å for X = F and 3.44 to 3.85 Å for X = I) below the sum of the van-der-Waals radii (P···F 3.36 Å, P···I 3.94 [19]). Since the halogens are oriented roughly opposite to a P–C bond (X···P–C 153 to 174°), these contacts might be taken as weak σ-hole interactions.[20] By analogy to **1a**$^+$,[15] the P–C$_{imi}$ distances in secondary cations exceed those in the imidazolio-phosphides **4b-e**[8b,c] but match the adjacent P–C$_{alkyl}$ distances (see Table 1). In view of this similarity, we address all P–C bonds in the cations **2**$^+$ and **5**$^+$ as single bonds.

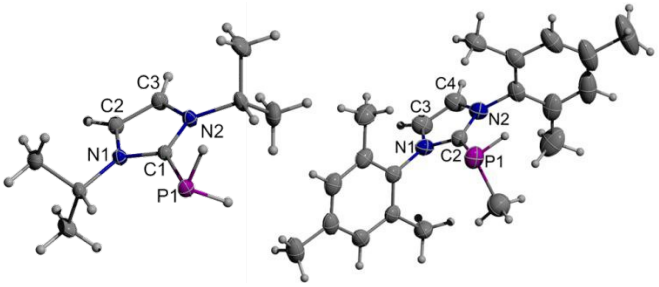

Figure 1: Molecular structure of the cations of **1d**[I] (left) and one of two crystallographically independent cations of **2c**[BF_4] (right) in the crystal. Thermal ellipsoids of heavy atoms were drawn at the 50% probability level. The P-bound hydrogen and methyl substituents of **2c**$^+$ are disordered over two positions, only one of which (with occupancy 0.75) is shown.

The ^{31}P NMR chemical shifts of cations (**1b-e**)$^+$ (δ^{31}P = -165.7 to -176.1) and (**2b-e**)$^+$ (δ^{31}P = -115.2 to -95.3) compare to those of primary or secondary methyl phosphines (δ^{31}P -163.5 for

$MePH_2$ and -99.5 for Me_2PH [21]) and the ^1H NMR data indicate that secondary cations **2**$^+$ and **5**$^+$ with N-*i*Pr- and N-Dipp-substituents are, like neutral phosphines, at ambient temperature configurationally stable on the NMR timescale. Based on their spectroscopic and structural features, we address cations **1**$^+$, **2**$^+$ and **5**$^+$ as imidazolio-substituted primary and secondary phosphines and consider them analogues of the well-known tertiary α-cationic phosphines that have received some attention in coordination chemistry and catalysis.[17]

Table 1. Selected distances for imidazolio-phosphines (**1a-e**)[X], (**2b,c**)[X], **3a**[BF_4], **5b**[BF_4], (**19a,c**)[BF_4] and imidazolio-alkylphosphides **6b**, **8b**.

	R^1	R^2	R^3	P–C_{imi}	P–C_{alkyl}
1a[OTf] [a]	Ar [b]	--	--	1.840(4)	--
1b[I]	Dipp [c]	--	--	1.845(7)	--
1b[BF_4]	Dipp [c]	--	--	1.816(4)	--
1c[I]	Mes	--	--	[e]	--
1d[I]	*i*Pr	--	--	1.825(2)	--
1e[I]	Me	--	--	1.83(2)	--
2b[I]	Dipp [c]	Me	--	1.837(3)	1.805(4)
2c[BF_4]	Mes	Me	--	1.828(3)	[e]
3a[BF_4] [a]	Ar [b]	CPh_3	--	1.845(2)	1.921(2)
5b[BF_4]	Dipp [c]	Et	--	1.828(2)	[e]
6b [f]	Dipp [c]	Et	--	1.770(4)	1863(4)
				1.757(4)	1.868(4)
8b	Dipp [c]	Me	--	1.750(2)	1.855(2)
19a[BF_4]	Dipp [c]	Me	Me	1.845(2)	1.823(2)
19c[BF_4]	Dipp [c]	Et	Me	1.843(2)	[e]

a) Data from ref. 15 b) Ar = 2,6-di-benzhydryl- 4-methyl-phenyl. c) Dipp = 2,6-di-isopropyl-phenyl. d) Mes = 2,4,6-trimethyl-phenyl. e) Unambiguous determination unfeasible due to crystallographic disorder. f) data for two crystallographically independent molecules.

Deprotonation of secondary imidazolio-phosphines.

The acid behaviour of secondary imidazolio-phosphines is best illustrated by the outcome of a screening of the reactivity of **5b**[BF_4] towards various bases. Analysis of $^{31}P\{^1H\}$ (Figure 2) and ^1H NMR spectra allowed us to establish in all reactions the formation of mixtures of imidazolio-ethylphosphide **6b**, cyclic oligophosphines $(EtP)_n$ (n = 3–5),**2**[a] and imidazolium ion **7b**$^+$.

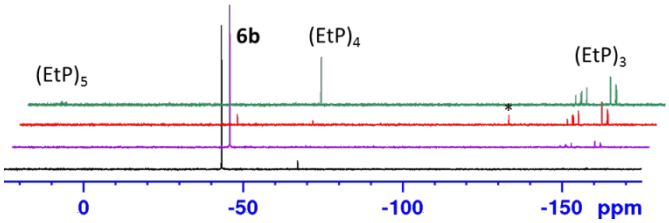

Figure 2: $^{31}P\{^1H\}$ NMR spectra of the reaction mixtures formed upon treatment of **5b**[BF_4] with KHMDS (black trace), LDA (purple trace), $NaBH_4$ (red trace) and Et_3N (green trace) in MeCN (* = unidentified product).

Analogous behaviour was also confirmed for (**2b-e**)[X] (X = I, BF_4) and led us to summarize the observed reactivity by the generic equation shown in Scheme 2. The products can be rationalized as arising from two competing reactions, viz. (i) deprotonation of the starting materials to afford **6b**, **8b-e** and (ii) cyclocondensation under P–P bond formation and cleavage of (**7b-e**)[X] to produce $(RP)_n$ (R = Me, Et; n = 3-5). We want to note that the combination of electrophilic alkylation and subsequent base-induced deprotonation provides a viable mechanistic explanation for previously observed electrophilic substitution reactions[8b,18] at primary imidazolio phosphide **4b**.

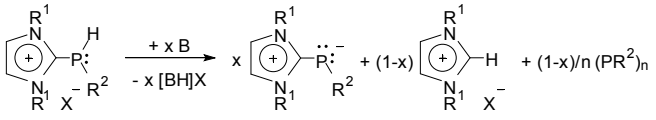

(**2b-e**)[X] (R^2 = Me) **8b-e** (R^2 = Me) (**7b-e**)[X] (R^2 = Me, Et;
5b[X] (R = Et) **6b** (R^2 = Et) n = 3 - 5)

Scheme 2: Generic equation describing the reaction of secondary imidazolio-phosphines (**2b-e**)[X], **5b**[X] with bases (X = I, BF_4; B = $N(SiMe_3)_2^-$, $NiPr_2^-$, *t*-BuO^-, H^-, BH_4^-, Et_3N; $0 \le x \le 1$).

The balance between both reaction channels is strongly influenced by the choice of the base. Deprotonation to yield **6b** is generally preferred with anion bases like potassium *tert*-butoxide (*t*-BuOK), potassium hexamethyldisilazide (KHMDS), potassium hydride (KH), or lithium diisopropylamide (LDA). The highest selectivity for **6b** (x > 0.9) was achieved with KHMDS, while the other anion bases gave less phosphide (x = 0.70 – 0.84) at the expense of an increased amount of $(EtP)_n$. Under synthetic aspects, *t*-BuLi performed similar to KHMDS when the reaction was carried out at low temperature, and its application enabled isolating crystalline samples of **6b** and **8b** in decent yields (58-65%). The molecular structures in the crystal (Figure 3, ESI) resemble those of known imidazolio-phosphides. The P-C_{imi} distances (1.750(2), 1.757(4) Å) match those in P–H- (1.752(1) to 1.772(1) Å [8]) or P–R-substituted congeners (R = Ph, CF_3, 1.763(6) to 1.794(3) Å[5b]), whereas the P–C_{alkyl} distances (1.855(2) to 1.868(4) Å) unexpectedly exceed that in cation **5b**$^+$ (1.805(4) Å). The ^{31}P NMR chemical shifts of **6b** and **8b** ($\delta^{31}P$ -61.4, -39.9 in THF-d_8) roughly match those of phenyl and CF_3-substituted analogues ($\delta^{31}P$ -23.0 to -53.4 [8b]).

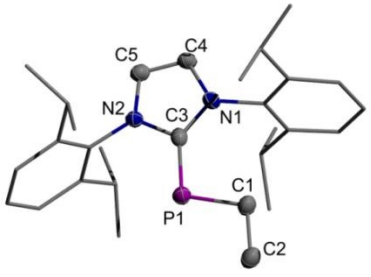

Figure 3: Molecular structure of one of two crystallographically independent molecules of **6b** in the crystal. For clarity, hydrogen atoms were omitted and N-Dipp substituents drawn using a wire model. Thermal ellipsoids were drawn at the 50% probability level. Only one of two positions of a disordered *i*Pr group (occupancy 0.682(14)) is shown.

Cyclic oligophosphines $(EtP)_n$ became the major products of the reaction of **5b**[BF_4] with sodium borohydride ($NaBH_4$), which was chosen as a more soluble hydride source than KH. Whilst imidazolio-phosphide **6b** was under these conditions still detected as a minor component (x = 0.09), exclusive formation of $(EtP)_n$ (x = 0) occurred when the reaction was

carried out using an equimolar amount of triethyl amine (Et_3N). Reaction monitoring revealed that $(EtP)_3$ and $(EtP)_4$ formed in this and in all other reactions studied as kinetically favoured cyclocondensation products. In contrast, $(EtP)_5$ is a secondary product that grew in later but became the dominant species in the final product mixture. The ring metathesis implied by these transformations was repeatedly reported in the literature[2a,22] and is driven by the decline in ring strain with increasing ring size. Because the rate of ring scrambling is slow compared to the consumption of starting material, we consider it a follow-up process that is unrelated to the initial base reaction of **5b**$^+$.

In accord with the equation in Scheme 2, which implies that the cyclo-condensation does not result in a net consumption of base, we established that quantitative formation of $(EtP)_n$ occurs as well upon exposure of **5b**$[BF_4]$ to a sub-stoichiometric quantity (approx. 10 mol-%) of Et_3N.[§] In view of the stability of base-free solutions of imidazolio-phosphines, these findings clearly identify the cyclocondensation as a base-catalysed process. Adopting this hypothesis, we reasoned that an imidazolio-phosphide should also be capable of initiating P–P bond formation. A first corroboration of this conjecture was obtained during attempts to optimize the protocol for alkylating **4b-e**. In particular, we noted that adding the imidazolio-phosphide to an excess alkylating agent gave high yields of imidazolio-phosphines **2**$^+$, **5**$^+$ while condensation to furnish (**7b-e**)$^+$ and $(RP)_n$ (R = Me, Et; n = 3-5) occurred with high selectivity, or even exclusively, when the addition of the reagents was reversed. We presume that the condensation is in the first case inhibited by immediate quenching of the imidazolio-phosphide by the electrophile, and in the second case promoted by attack of a local excess of still unreacted **4b-e** on the cationic alkyl phosphine formed. The ability of **6b** to catalyse the condensation of **5b**$^+$ to yield $(PEt)_n$ and **7b**$^+$ was confirmed by independent control experiments (see ESI).

Monitoring the progress of the reaction of **5b**$[BF_4]$ with a catalytic amount of **6b** (17 mol-%) at -35 °C by NMR spectroscopy enabled further casting some light on the formation mechanism of the cyclic oligophosphines. We found that cationic **5b**$^+$ is nearly instantly transformed into a mixture of transient intermediates, which then decay slowly at -35 °C and more rapidly and quantitatively at ambient temperature to afford $(PEt)_n$ as the final products. Assessment of the $^{31}P\{^1H\}$ NMR spectra (see Figure 4 and ESI) allowed decomposing the signals of transient species into two AX- and four ABX-type patterns attributable to newly formed di- and triphosphines. Identification of the diphosphines as the two diastereomers of **9**$^+$ (Chart 2) was derived from ^{31}P and $^1H,^{31}P$ HMQC spectra, which confirmed the presence of two ethyl-, a hydrogen- and an imidazolio-substituent on the P_2-unit (see ESI). Similar analysis of the signals attributed to transient triphosphines indicated that all phosphorus atoms are alkylated and one carries an additional proton, and we assign these species thus as the four possible diastereomers of **10**$^+$. Monitoring the progress of the reaction over time revealed that the concentration of **9**$^+$ rises and decays more rapidly than that of **10**$^+$, whereas the amount of imidazolio-phosphide does not vary significantly during the whole period.

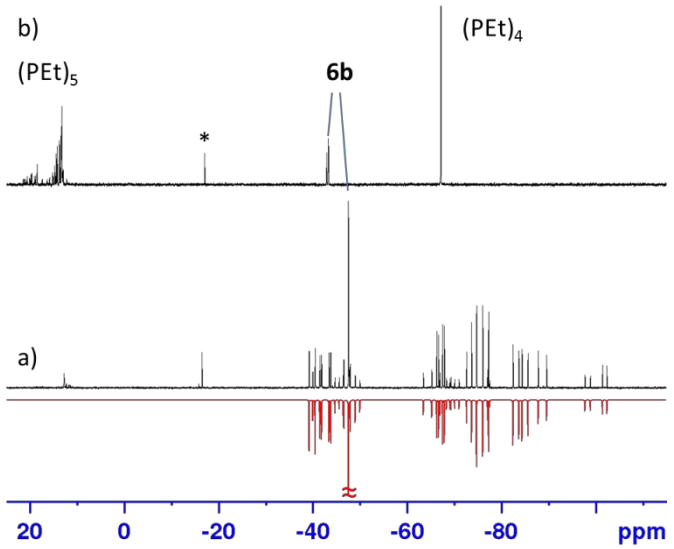

Figure 4: Expansion of the $^{31}P\{^1H\}$ NMR spectra of a mixture of **5b**$[BF_4]$/**6b** (5:1) in CD_3CN a) after 6 h reaction time at -35 °C, b) after 7 d at ambient temperature. The red trace is the result of a simulation of the low-frequency region as a superposition of the signals of the reactants, $(PEt)_4$, and two AX and three ABX signal patterns of transient di- and triphosphines (see ESI for details). Note that the signal of **6b** in b) is shifted because of a marked temperature dependence and split into several lines as a consequence of H/D-exchange with the solvent. The asterisk denotes the signal of an impurity present during the whole reaction.

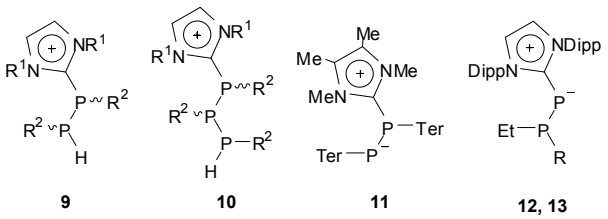

Chart 2: Proposed molecular structures of di- and triphosphine intermediates **9**$^+$, **10**$^+$ (R^1 = Dipp, R^2 = Et), **12** (R = H), **13** (R = PHEt, 2 diastereomers) and diphosphene-carbene adduct **11**[23] (Ter = 2,6-$Mes_2C_6H_3$).

Altogether, these findings imply that **5**$^+$ reacts first via stepwise chain elongation to yield linear di- and triphosphines, which then cyclize to the final products. The absence of any P_1-building block other than **6b** during the later stages of the reaction suggests strongly that the imidazolio-phosphide is engaged in the chain elongation process, and the persistence of this species at the end of the reaction substantiates that this engagement is catalytic. It should be noted that **9**$^+$ is a congener of the conjugate acid of a zwitterion **11** (Chart 2) that has been addressed as NHC-adduct of a diphosphene and reacts with H_2O under cleavage of the carbene and hydration of the resulting PP double bond rather than undergoing protonation to an analogue of **9**$^+$.[23] The different behaviour is presumably caused by the steric encumbrance imposed by the bulky terphenyl groups in **11**, which induce a marked weakening of the bond connecting the P_2 and imidazole units.

Observations made during studies on the electrophilic methylation of **4e** prompted us to study also the suitability of a primary imidazolio-phosphide as catalyst for condensation

View Article Online
DOI: 10.1039/D0DT03673A

processes. Monitoring titrations of **4b** with **5b**[BF_4] by ^{31}P NMR spectroscopy, we found that addition of a sub-stoichiometric amount of reagent resulted in formation of **6b** along with a new product identified spectroscopically as imidazolio-diphosphide **12** (Chart 2). Action of more than one equivalent of **5b**$^+$ on **4b** gave rise to detectable amounts of **9**$^+$ and **10**$^+$, which rapidly decayed to produce $(PEt)_n$ (n = 3-5), and to a yet unobserved triphosphine assigned as **13** (Chart 2, two diastereomers). The signals of **12** and **13** decayed eventually, leaving $(PEt)_n$ and imidazolio-phosphides **4b**, **6b** as the only persistent phosphorus-containing reaction products.

The outcome of the titration experiments shows that the cyclocondensation is mechanistically more complex when **4b** rather than **6b** is used as catalyst. The detection of **6b**, which is obviously produced by deprotonation of **5b**$^+$ at an early stage, and transient **9**$^+$, **10**$^+$ implies that the previously discussed route to $(EtP)_n$ is still viable. The available data allow no decision if the new transient species (**12**, **13**) are involved in an alternative or possibly competing pathway leading to $(EtP)_n$ or merely in a reversible but 'unproductive' side reaction.[§§]

Deprotonation of primary imidazolio-phosphines.

A dichotomy between proton transfer and P–P bond formation was also established for the base-reactions of primary cationic phosphines (**1b-e**)$^+$. Condensation and cleavage of imidazolium salts can be induced, as in the case of **2**$^+$ and **5**$^+$, by addition of catalytic quantities of Et_3N or an imidazolio-phosphide **4b-e** (10–30 mol-%),[§] or by stockpiling active reaction mixtures with additional cationic phosphine. All reactions proceed rapidly at ambient temperature to furnish mixtures of soluble linear phosphines P_nH_{n+2} (n = 1–3)[2,24] and intractable reddish precipitates. The composition of the solids could not be elucidated, but their colour suggests the presence of P_n-frameworks as in red phosphorus or insoluble polyphosphides. Added imidazolio-phosphide was not immediately consumed in the condensation, but disappeared during ageing of reaction mixtures, presumably via an undisclosed follow-up reaction.

Targeted deprotonation of a primary imidazolio-phosphine occurred, as in the case of (**2b-e**)$^+$, upon addition of the cationic phosphines to solutions of strong anion bases like KHMDS or *t*-BuOK, respectively. Formation of varying amounts of phosphine (PH_3) as by-product suggests, however, that condensation is not completely suppressed.[†]

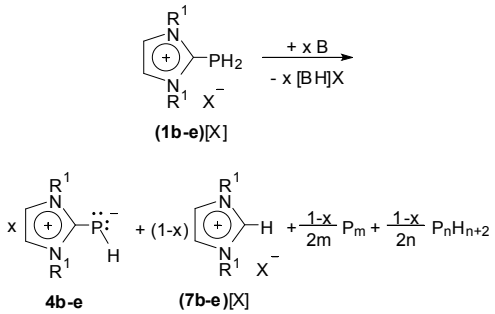

Scheme 3: Generic equation describing the reaction of primary imidazolio-phosphines (**1b-e**)[X], **5b**[X] with bases (X = I, BF_4; B = $N(SiMe_3)_2^-$,*t*-BuO^-, Et_3N; n = 1 – 3, 0 ≤ x ≤ 1).

As in the case of the secondary congeners, we can summarize the two-sided reactivity of **1b-e**[X] in a single generic equation (Scheme 3). Note that the condensation yields in this case no cyclic oligophosphines, but proceeds as a dismutation to afford a mixture of "hydrogen-rich" linear phosphines and "hydrogen-poor" insoluble polyphosphorus compounds of still unknown composition (the formulation as neutral P_m was made to ensure a correct stoichiometric balance and is not intended to represent the actual composition). The dismutation consumes no base and can thus be initiated by a catalytic amount of an imidazolio-phosphide or an external base like Et_3N.

NMR-spectroscopic monitoring of the reaction of **1d**[BF_4] with Et_3N in acetonitrile at -60 °C revealed the presence of transient intermediates beside the persistent products observable at room temperature. Simulation of $^{31}P\{^1H\}$ NMR spectra and comparison with literature data[2] allowed us to identify the prevailing intermediates as linear tetra- and pentaphosphines and cyclopentaphosphine $(PH)_5$ (see ESI; the composition of further minor species stays unknown). The signals of higher oligophosphines (P_nH_m with n > 3) broadened and decayed rapidly when the temperature was raised. Triphosphine P_3H_5 remained visible for some time at ambient temperature, but decomposed eventually to produce P_2H_4 and PH_3. Base-induced dismutation of higher oligophosphines P_nH_m is long established,[2] and we consider its observation in the present case once more a follow-up process that is unconnected with the initial reaction of **1d**$^+$. Regardless of our failure to detect any imidazolio-substituted oligophosphines, we presume that the observed P_n-frameworks are formed in a similar manner as in the condensation of secondary imidazolio-phosphines.

Computational Studies and mechanistic considerations.

To gain a deeper understanding of the P–P bond formation processes, we set out to model the behaviour of the sterically least protected imidazolio-phosphine **1e**$^+$ computationally. DFT calculations were carried out at the B3LYP-D3BJ/def2-tzvp//B3LYP-D3BJ/def2-svp level of theory, which reliably reproduces the experimentally observed structural features of **4e** and cations **1e**$^+$, **5e**$^+$. Solvation effects were simulated using a polarizable continuum model (PCM) with solvent parameters for THF. Anions of salt-like reactants were neglected to cut down the computational cost.

Starting with an account of the energetics of possible reactions of **1e**$^+$ (or (**15-P$_0$**)$^+$, Scheme 4) with imidazolio-phosphide **4e** (or **14-P$_0$**), we predict the degenerate proton transfer between both reactants (eqn. $(1)_{n=0}$, ΔG^0_{298} = 0.0 kcal mol^{-1}) as thermodynamically less favourable than condensation to give imidazolio-diphosphide **14-P$_1$** (eqn. $(2)_{n=0}$, ΔG^0_{298} = -5.8 kcal mol^{-1}, see Table 2). The negative Gibbs free energy of proton transfer from **1e**$^+$ to **14-P$_1$** (eqn. $(1)_{n=1}$, ΔG^0_{298} = -2.1 kcal mol^{-1}) identifies the latter as a slightly stronger base than **4e**. The products formed in such a step – diphosphine (**15-P$_1$**)$^+$ and **4e** – may undergo further condensation to furnish an imidazolio-triphosphide **14-P$_2$** (eqn. $(2)_{n=1}$, ΔG^0_{298} = -6.4 kcal mol^{-1}), which is the thermodynamically preferred phosphorus-containing product of the reaction between **4e** and two cations **1e**$^+$. In a similar manner, further reaction of **14-P$_2$** with **1e**$^+$ under

proton transfer (eqn. (1)$_{n=2}$, ΔG^0_{298} = -5.5 kcal mol^{-1}) and exergonic condensation (eqn. (2)$_{n=2}$, ΔG^0_{298} = -13.6 kcal mol^{-1}) may afford tetraphosphide **14-P$_3$**. This species is obviously slightly less basic than **4e** (see Table 2), but exergonic chain extension (eqn. (2)$_{n=3}$, ΔG^0_{298} = -7.1 kcal mol^{-1}) remains still feasible. Formation of chains with more than five phosphorus atoms was not investigated, but seems conceivable as well.

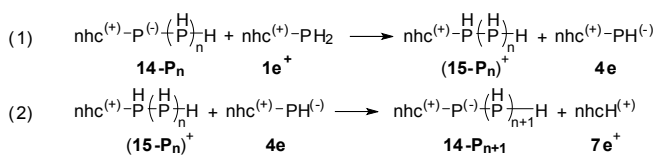

Scheme 4: Generic equations describing the proton transfer between imidazolio-(oligo)phosphides **14-P$_n$** and **1e$^+$** (eqn. (1)) and condensation of the resulting products (**15-P$_n$**)$^+$ and **4e** to yield chain-extended imidazolio-oligophosphides (eqn. (2)). Note that **4e** and **1e$^+$** can also be denoted as **14-P$_0$** and (**15-P$_0$**)$^+$, respectively. Calculated standard Gibbs free energies ΔG^0_{298} are listed in Table 2. For brevity, 1,3-dimethylimidazolio-fragments are represented as "nhc$^{(+)}$".

Table 2. Standard Gibbs free energies ΔG^0_{298}(in kcal mol^{-1}) for the reactions in Schemes 4, 5 computed at the PCM(THF)-B3LYP-D3BJ/def2-tzvp//PCM(THF)-B3LYP-D3BJ/def2-svp level of theory.

	reaction						
n	(1)	(2)	m	(3)[a]	(4)[a]	(5)[b]	(6)
0	0.0	-5.8	1	-5.8 (-5.8)	-7.9 (-7.9)		
1	-2.1	-6.4	2	-12.2 (-6.1)	-17.7 (-8.8)	-23.7 (-6.0)	
2	-5.5	-13.6	3	-25.8 (-8.6)	-25.5 (-8.5)	-32.1 (-6.7)	-37.6
3	0.3	-7.1	4	-32.9 (-8.2)	-32.6 (-8.1)	-54.2 (-21.6)	-45.3
4	0.3						

a) values in parentheses denote the average gain in ΔG^0_{298} per P–P bond formed (ΔG^0_{298},avg = ΔG^0_{298}/y). b) values in parentheses denote ΔG^0_{298} of the ring closure step nhc$^{(+)}$-(PH)$_y$-PH$_2$ → (PH)$_{y+1}$ + nhcH$^{(+)}$.

Taken together, the individual reaction steps discussed so far describe in principle a reaction cascade for the assembly of linear oligophosphines by sequential chain-elongation steps. The Gibbs free energies of the gross reactions, which can be represented as condensations of **4e** with different amounts of imidazolio-phosphine **1e$^+$** (eqn. (3), Scheme 5), indicate that formation of P$_n$-chains is thermodynamically favourable. The average gain in free energy per P–P bond formed increases from ca. 6 kcal mol^{-1} for **14-P$_1$** and **14-P$_2$** to some 8 kcal mol^{-1} for tetra- and pentaphosphines **14-P$_3$** and **14-P$_4$**, respectively.

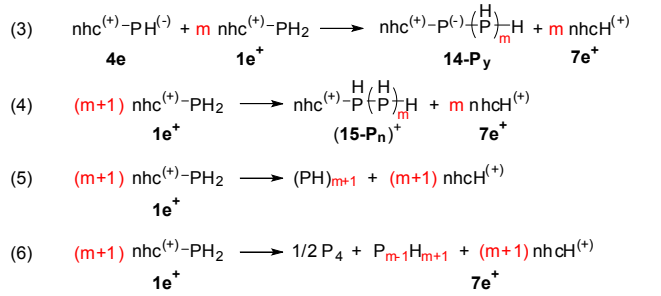

Scheme 5: Gross reactions describing formation of linear imidazolio-oligophosphides **14-P$_n$** (eqn. (3)) and –oligophosphines (**15-P$_m$**)$^+$ (eqn. (4)), cyclic oligophosphines (PH)$_{m+1}$ (eqn. (5)) and dismutation products (P$_4$ and P$_2$H$_4$/P$_3$H$_5$, eqn. (6), m = 3, 4) by condensation of **1e$^+$** or **1e$^+$/4b**, respectively. Note that the phosphorus atom count in all reactions is m+1. Calculated standard Gibbs free energies ΔG^0_{298} are listed in Table 2. For brevity, 1,3-dimethylimidazolio-subsitituents are denoted as "nhc$^{(+)}$".

An intriguing aspect turns up when we combine the formation of **14-P$_n$** from **4e** and **1e$^+$** embodied by eqn. (3) with subsequent protonation of the resulting zwitterion by one more molecule of **1e$^+$**. Imidazolio-phosphide **4e** consumed in the first reaction is then recovered and adopts thus the role of a catalyst, and the overall reaction can be represented according to eqn. (4) as condensation of imidazolio-phosphines **1e$^+$** to yield oligophosphines (**15-P$_n$**)$^+$ and an appropriate amount of **7e$^+$**. The Gibbs free energies indicate that formation of di- and triphosphines (**15-P$_2$**)$^+$ and (**15-P$_3$**)$^+$ is associated with an even larger (by 2 to 3 kcal mol^{-1}) driving force than assembly of the zwitterions **14-P$_2$**, **14-P$_3$**, whereas the differences level out for cationic and neutral tetra- and pentaphosphorus species.

Cyclic oligophosphines (PH)$_n$ (n = 3-5) can be formally obtained by an additional exergonic ring-closing condensation of linear tri- to penta-phosphines (ΔG^0_{298} = -6.0, -6.6 and -21.6 kcal mol^{-1} for three- to five-membered rings, Table 2), which renders the products thermodynamically more stable than linear oligophosphines with the same number of phosphorus atoms. The low Gibbs free energies for ring-closure to (PH)$_3$ and (PH)$_4$ mirror obviously the ring strain in the products,[2,22] while formation of (PH)$_5$ benefits from a strong driving force.

Last, but not least, we looked also into the energetics of reactions producing P$_2$H$_4$ and P$_3$H$_5$. Assuming formation of P$_4$ as by-product, producing these species from **1e$^+$** according to eqn. (6) is likewise thermodynamically favoured over simple condensation to linear imidazolio-oligophosphines (Table 2). The driving force ΔG^0_{298}(dismut) for creation of the final products through formal dismutation of a linear precursor (**15-P$_m$**)$^+$ (m = 4, 5) is measured by the difference in ΔG^0_{298} of eqns. (6) and (4). The calculated values of -12.4 and -12.7 kcal mol^{-1} associated with the generation of P$_2$H$_4$ and P$_3$H$_5$, respectively, are more negative than the Gibbs free energies for ring closure steps yielding (PH)$_3$ and (PH)$_4$ (Table 2; note that (PR)$_{3,4}$ (R = Me, Et) are the kinetic products resulting from condensation of **2b$^+$** and **5b$^+$**), but do not reach the level predicted for formation of (PH)$_5$. It must be borne in mind, however, that the dismutation energetics depends decisively on the nature of the "hydrogen-poor" co-product. Since the reaction becomes more exergonic when a more stable phosphorus allotrope than P$_4$ is formed, the values of ΔG^0_{298}(dismut) represent only thresholds, and an absolute assessment remains unfeasible as long as the co-product cannot be specified.

Having demonstrated the thermodynamic feasibility of various condensation processes, we also wanted to elucidate viable kinetic pathways. To this end, we set out to identify transition states for key reaction steps, starting with the interaction between imidazolio-phosphide **4e** and cationic phosphine **1e$^+$**. Probing various approaches of the reactants, we could locate transition states for two reaction channels. The molecular geometry of TS 1 (Figure 5) features a nearly symmetric P···H···P array and spawns the degenerate proton transfer between both reactants (eqn. (1) with n = 0). A low Gibbs free activation

energy ($\Delta G^{\neq}_{298}$= 7.1 kcal mol^{-1}) for this process is well in accord with rapid proton scrambling at ambient temperature.

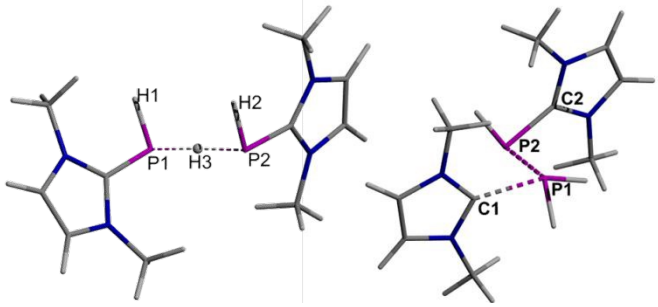

Figure 5: Computed (PCM(THF)-B3LYP-D3BJ/def2-tzvp//PCM(THF)-B3LYP-D3BJ/def2-svp) molecular geometries of transition states **TS1** (left) and **TS2** (right) for different reactions between **1e**$^+$ and **4e**. Selected distances (in Å): **TS1**: H1–P1 1.422, P1–H3 1.757, H3–P2 1.756, P2–H2 1.422; **TS 2**: C1–P1 2.087, P1–P2 2.453, P2–C2 1.817

Transition state TS2 embodies the energetically highest point on the reaction coordinate of a substitution process and is noteworthy for two aspects. First, the coordination geometry at the reaction centre deviates from the common (pseudo) trigonal-bipyramidal pattern in which incoming and leaving groups occupy axial positions, and appears rather as tetragonal pyramidal with a phosphorus lone-pair adopting the axial and the exchanging substituents adjacent basal positions. Second, both exchanging groups (imidazolio-phosphide and NHC) are not charged but neutral, rendering the whole process more similar to a ligand displacement at a metal complex[25] than a typical substitution in an element-organic molecule.

At first glance, the coupling of **4e** and **1e**$^+$ under P–P bond formation and expulsion of NHC **16e** associated with TS2 (eqn. (7), Scheme 6) is predicted to be distinctly endergonic (ΔG^0_{298} = +10.9 kcal mol^{-1}). However, the strongly basic carbene may abstract a proton from the coupling product (**15-P$_1$**)$^+$ (eqn. (9), ΔG^0_{298} = -16.7 kcal mol^{-1}) or a second molecule of **1e**$^+$ (eqn. (8), ΔG^0_{298} = -18.8 kcal mol^{-1}) without the need to pass an energetic barrier. The last alternative is more exergonic, and concatenation of P–P-coupling and proton transfer results in an overall exergonic condensation (eqn. (10), ΔG^0_{298} = -7.9 kcal mol^{-1}) representing the first chain-extension step of the gross reaction described by eqn. (4) with m = 1.

(7) $\underset{\mathbf{1e}^+}{nhc^{(+)}\text{-}PH_2} + \underset{\mathbf{4e}}{nhc^{(+)}\text{-}PH^{(-)}} \longrightarrow \underset{(\mathbf{15\text{-}P_1})^+}{nhc^{(+)}\text{-}\overset{H}{P}\text{—}PH_2} + \underset{\mathbf{16e}}{nhc}$

(8) $\underset{\mathbf{16e}}{nhc} + \underset{\mathbf{1e}^+}{nhc^{(+)}\text{-}PH_2} \longrightarrow \underset{\mathbf{7e}^+}{nhcH^{(+)}} + \underset{\mathbf{4e}}{nhc^{(+)}\text{-}PH^{(-)}}$

(9) $\underset{(\mathbf{15\text{-}P_1})^+}{nhc^{(+)}\text{-}\overset{H}{P}\text{—}PH_2} + \underset{\mathbf{16e}}{nhc} \longrightarrow \underset{\mathbf{14\text{-}P_1}}{nhc^{(+)}\text{-}P^{(-)}\cdot PH_2} + \underset{\mathbf{7e}^+}{nhcH^{(+)}}$

(10) $2\ \underset{\mathbf{1e}^+}{nhc^{(+)}\text{-}PH_2} \longrightarrow \underset{(\mathbf{15\text{-}P_1})^+}{nhc^{(+)}\text{-}\overset{H}{P}\text{—}PH_2} + \underset{\mathbf{7e}^+}{nhcH^{(+)}}$

Scheme 6: Elementary reaction steps involving nucleophile-induced P–P bond formation under expulsion of a carbene (eqn. (7)) and carbene protonation by **1e**$^+$ (eqn. (8)) or (**15-P$_1$**)$^+$ (eqn. (9)). Combining eqns. (7) and (8) adds up to a condensation of two molecules of **1e**$^+$, eqn. (10). 1,3-Dimethylimidazolio-fragments are denoted as "nhc$^{(+)}$".

While a chain growth mechanism implied by eqn. (10) is at first glance compatible with our experimental findings, the Gibbs free energy of activation ($\Delta G^{\neq}_{298}$(TS2) = 32.9 kcal mol^{-1}) seems hardly compatible with an instantaneous reaction of primary cationic phosphines (**1b-e**)$^+$ under ambient conditions (note that these species react obviously too fast to render diphosphine intermediates observable by NMR). A solution to this dilemma emerged when we studied possible interactions between NHC **16e** and cationic diphosphine **15-P$_1$**. Simulation of different approaches of the reactants allowed us to identify once again two reaction channels. The first one represents the aforementioned proton transfer to the NHC (eqn. (9)). The second transformation reverses reaction (7), but differs from the route via TS2 in following a "regular" pathway in which the NHC approaches from a direction opposite to the P–P bond to be cleaved (Figure 6). Intriguingly, our calculations depict both processes as barrier-less transformations that do not require traversing a transition state. Recurring to the concept of microscopic reversibility, the "forward" reaction (7) of **1e**$^+$ and **4e** to yield imidazolio-diphosphine (**15-P$_1$**)$^+$ and **16e** can then likewise be considered barrier-less.

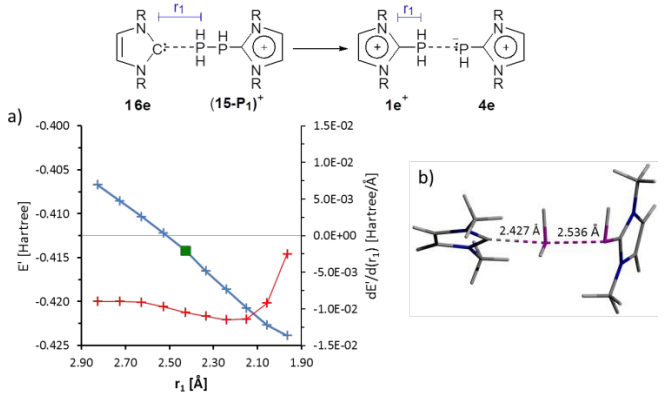

Figure 6: Results of a relaxed potential energy surface scan (at the B3LYP-D3BJ/def2-svp level) for the reaction between **16e** and (**15-P$_1$**)$^+$ to give **1e**$^+$ and **4e** using C(NHC)···P vector r_1 as independent variable. (a) Plot of the reduced electronic energy E' = E + 1293 Hartree (blue) and its derivative dE'/dr$_1$ (red) vs. r_1. (b) Computed molecular geometry at an intermediate scan point (r_1 = 2.427 Å, marked with a green square).

Similar pathways as for the reaction of **4e** with **1e**$^+$ were identified for selected chain growth steps yielding imidazolio-oligophosphines (**15-P$_n$**)$^+$ (n = 2 - 4) from **4e** and appropriate precursors (**15-P$_{n-1}$**)$^+$. We therefore suggest describing the P–P bond forming condensations of two cationic phosphines **1e**$^+$ as exemplified by eqn. (10) and the analogous reactions of one molecule of **1e**$^+$ with a homologue (**15-P$_{n-1}$**)$^+$ generally as two-step processes that are catalysed by imidazolio-phosphide **4e**. The first step involves nucleophilic attack of **4e** on a cationic phosphine (**1e**$^+$ or (**15-P$_{n-1}$**)$^+$) under liberation of an NHC and represents a Lewis-acid/base reaction mimicking the ligand substitution in a metal complex. In the second step, the NHC is sequestered by Brønsted-type proton transfer from **1e**$^+$ (note that this reaction may compete for higher oligophosphines (**15-P$_n$**)$^+$ (n = 3, 4) with the deprotonation of the condensation product). Both reaction steps require passing only low energy barriers, or may even proceed without a barrier.

Formation of the simplest cyclic oligophosphine $(PH)_3$ might in principle occur by ring closure of cationic triphosphine $(\mathbf{15\text{-}P_2})^+$ under cleavage of imidazolium ion $\mathbf{7e}^+$, but our failure to locate a suitable transition state renders this pathway unlikely. Gratifyingly, we found that the target product can be accessed via exergonic ring-closing fragmentation of a tetraphosphide **17-P₃** (eqn. (11), Scheme 7, ΔG^0_{298} = -14.9 kcal mol^{-1}) arising from deprotonation of the terminal PH_2-unit of cation $(\mathbf{15\text{-}P_3})^+$ by a transient NHC. This reaction branch has a similar driving force (ΔG^0_{298} = -18.1 kcal mol^{-1}) as barrier-less quenching of the NHC by $\mathbf{1e}^+$ (eqn. (8), ΔG^0_{298} = -18.8 kcal mol^{-1}) but is kinetically less favoured ($\Delta G^{\neq}_{298}$ = +9.3 kcal mol^{-1}). Accumulation of the cyclotriphosphine as a major product is thus deemed unlikely. Nonetheless, an analogous reaction allows explaining the formation of alkylated cyclotriphosphines $(PR)_3$ (R = Me, Et) from imidazolio-tetraphosphines $nhc^{(+)}$-$(PR)_3$-PHR, where deprotonation at the remote phosphorus atom (relative to the imidazolio-substituent) is the only feasible reaction mode.

(11) $nhc^{(+)}\{(H)(P)_3PH^{(-)}\}$ → $(PH)_3$ + $nhc^{(+)}$–$PH^{(-)}$

17-P₃ **4e**

Scheme 7: Ring-closing fragmentation of tetraphosphide **17-P₃**. For brevity, 1,3-dimethylimidazolio-fragments are represented as "$nhc^{(+)}$".

Finally, we succeeded in elaborating model reactions leading to P_2H_4 and P_3H_5 (Scheme 8). The key is the creation of specific stereoisomers of zwitterionic tri- and tetraphosphides **18-R** (R = H, PH_2) with a phosphide unit in γ-position to the imidazolio group. These species have distinctly lengthened P_α–P_β bonds (Figure 7a) and can like **11**[23] be viewed as charge-transfer complexes of elusive diphosphenes HP=PR (R = H, PH_2) with **4e**. Their reaction with imidazolio-oligophosphide **14-P₂** (or higher congeners) proceeds under formal dihydrogen transfer to the diphosphene unit (see Figure 7b) to afford **4e**, oligophosphines H_2P–PHR (R = H, PH_2), and a new diphosphene that is assumed to be kinetically unstable and to decay in follow-up reactions that were not analysed further.

(12) $nhc^{(+)}$–P(H)–P(H)–$P^{(-)}$–R (**18-R**) + $nhc^{(+)}$–$P^{(-)}$–P(H)–PH (**14-P₂**) → $nhc^{(+)}$–$PH^{(-)}$ (**4e**) + HP(H)–P(H)–R + [$nhc^{(+)}$–$P^{(-)}$=PH] → follow-up reactions

Scheme 8: Model reaction describing formation of P_2H_4 (R = H) and P_3H_5 (R = PH_2) from transient zwitterions **18-R**. 1,3-Dimethylimidazolio-fragments are denoted as "$nhc^{(+)}$".

The oligophosphides **18-R** can be created by NHC-induced deprotonation of phosphines $(\mathbf{15\text{-}P_2})^+$ and $(\mathbf{15\text{-}P_3})^+$, even if they are less stable than their tautomers **14-P₂** ($\Delta\Delta G^0_{298}$(**18-H**) = 5.8 kcal mol^{-1}) and **14-P₃** ($\Delta\Delta G^0_{298}$(**18-PH₂**) = 7.7 kcal mol^{-1}), respectively. Alternatively, **18-H** can form in a balanced (ΔG^0_{298} ≈ 0) barrier-less reaction through NHC-induced fragmentation of an imidazolio-pentaphosphine $(\mathbf{15\text{-}P_4})^+$ (see ESI). Generation of P_2H_4 and P_3H_5 from **18-R** and **14-P₂** requires passing moderate kinetic barriers ($\Delta G^{\neq}_{298}$ = 17.6 , 15.5 kcal mol^{-1}).

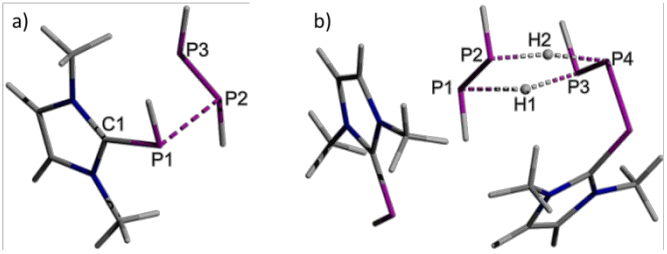

Figure 7. Computed (PCM(THF)-B3LYP-D3BJ/def2-tzvp//PCM(THF)-B3LYP-D3BJ/def2-svp) molecular structures of a) **18-H**, b) the transition state of the reaction between **18-H** and **14-P₂** leading to the formation of P_2H_4. Selected distances (in Å): **18-H**: C1–P1 1.803, P1–P2 2.485, P2–P3 2.125; TS(**18H** + **14-P₂**): P1–P2 2.127, P3–P4 2.163, P1–H1 2.001; H1–P3 1.543, P2–H2 1.615, H2–P4 1.773.

A preliminary exploration of the reactions between secondary cationic phosphine $\mathbf{2e}^+$ and its conjugate phosphide **8e** (see ESI) reveals that coupling to yield a methylated analogue of $\mathbf{9}^+$ (Chart 2, R^1 = R^2 = Me) and an NHC is less endergonic (ΔG^0_{298}= 2.7 kcal mol^{-1}) and ensuing protonation of the carbene by a further molecule of $\mathbf{2e}^+$ less exergonic (ΔG^0_{298} = -9.0 kcal mol^{-1}) than the corresponding reactions of $\mathbf{1e}^+$ and **4e** (eqns. (7), (8), see Table 2). However, because both effects largely cancel each other out, the Gibbs free energy for the condensation of two secondary phosphines $\mathbf{2e}^+$ (ΔG^0_{298}= -6.2 kcal mol^{-1}) closely matches the value established for the coupling of the primary homologues $\mathbf{1e}^+$ (eqn. (10), ΔG^0_{298}= -5.8 kcal mol^{-1}), and falls also below that of the degenerate proton transfer between $\mathbf{2e}^+$ and **8e**. Moreover, identification of a permethylated (R^1 = R^2 = Me) analogue of **12** as most favourable P–P coupling product accessible from $\mathbf{2e}^+$ and **4e** is in accord with the observed formation of **12** during reaction of **2b** with **4b** (vide supra).

In total, the computational studies suggest that the complex reaction patterns of primary and secondary imidazolio-phosphines and the conjugate phosphides can be delineated into sequences of elementary steps in which the protagonists act either as Brønsted-acids or bases in proton transfer events, or as Lewis acids or bases (or electrophiles and nucleophiles) in reactions involving formation or breakage of a P–P bond. All steps are characterized by low-energy transition states, or may even proceed without energetic barriers. These preconditions enable smooth reactions at ambient conditions and flexible concatenation of several elementary steps to more complex transformations, which finally sum up to a diverse network that can be treated as one system of mutually coupled dynamic equilibria. The outcome of a reaction is in this setting controlled by thermodynamics, and the composition of any equilibrium mixture can easily be modified by changing the stoichiometric boundary conditions, e.g. by adding reagents. Moreover, the calculations allow also identify possible reaction pathways, which explain both the sequential formation of linear imidazolio-oligophosphines and the generation of cyclic oligophosphines (represented by $(PH)_3$ in the computational model) and P_2H_4/P_3H_5 as preferred final products (Figure 8).

View Article Online
DOI: 10.1039/D0DT03633A

ARTICLE

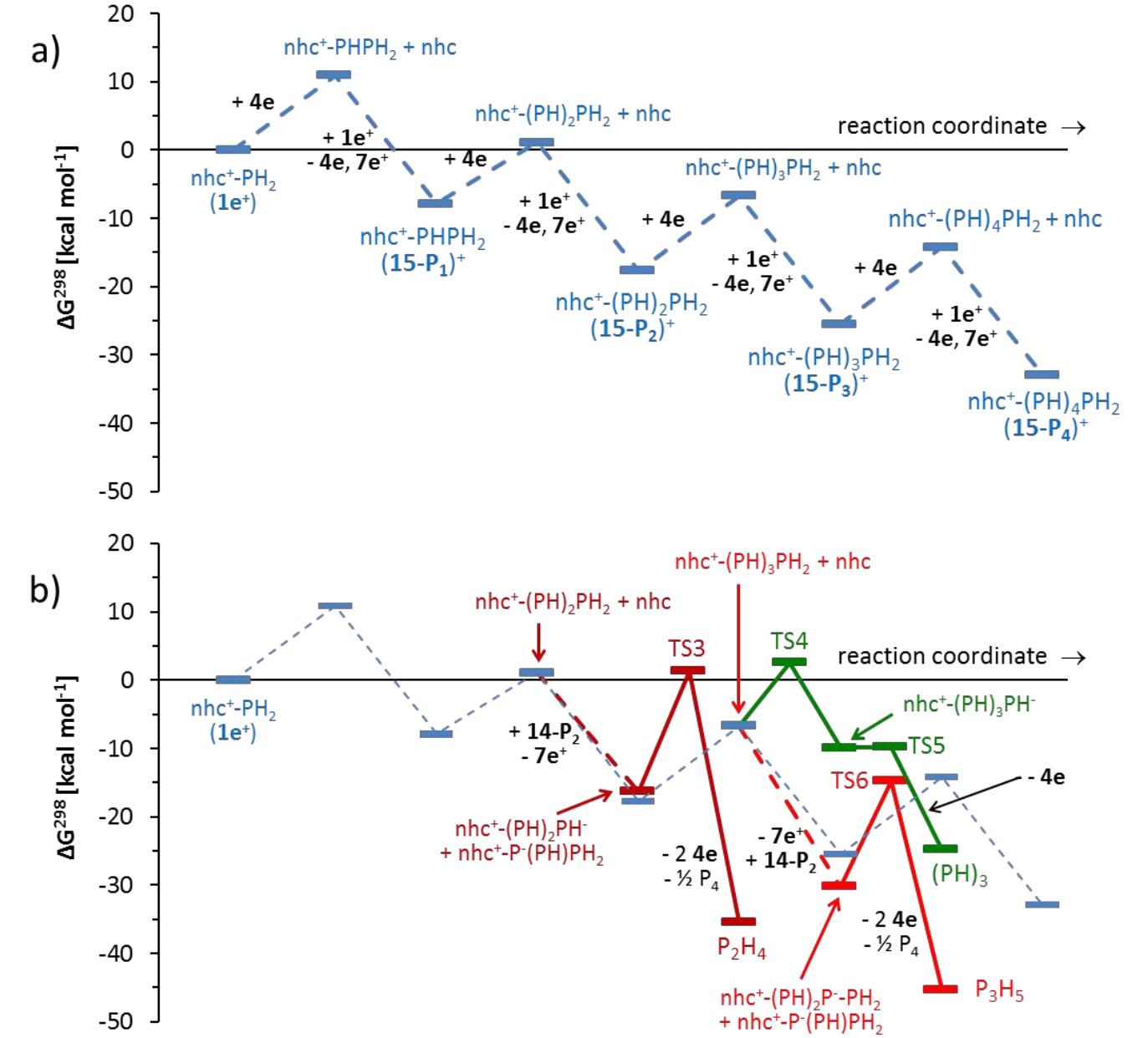

Figure 8. Computed (PCM(THF)-B3LYP-D3BJ/def2-tzvp//PCM(THF)-B3LYP-D3BJ/def2-svp) minimum energy reaction pathways illustrating (a) the stepwise assembly of linear imidazolio-oligophosphines (**15-P$_n$**)$^+$ (n = 2–4) by condensation of (**15-P$_{n-1}$**)$^+$ with **1e**$^+$ in the presence of **4e** as catalyst, (b) ring closure and dismutation reactions leading to $(PH)_3$ (in green) and P_2H_4/P_3H_5 (in dark/light red) respectively. Dashed lines denote transformations that may proceed according to relaxed potential energy scans without energy barriers.

The computational modelling reveals some corollaries that help understanding the factual reactivity of primary and secondary imidazolio-phosphines and -phosphides. First of all, any direct encounter of specimens of both types can give rise to two different reaction modes, viz. (i) Brønsted-type proton transfer and (ii) P–P bond forming condensation. The second pathway is generally more favourable and proceeds in two steps via an initial Lewis-type bond formation reaction and ensuing protonation of the concurrently created NHC by an imidazolio-phosphine with release of an imidazolium ion (eqns. (7) to (9), Scheme 6). The exergonic second step delivers the energy input that propels the endergonic first step and affords

a net driving force for the whole process. Moreover, it regenerates an imidazolio-(oligo)phosphide and enables thus the reaction to proceed in an autocatalytic and repetitive manner to form chains of P–P bonds. A practical consequence of this autocatalysis is that specific alkylation of imidazolio-phosphides to produce secondary cationic phosphines and deprotonation of the latter to yield P-alkylated imidazolio-phosphides are only feasible when the coexistence of both contestants is avoided, e.g. by rapid quenching of initial reactants with an efficient alkylating agent or a strong base.

Our DFT studies allow also some comments on the role of NHCs in the reaction network. First of all, the substitution step compares to known reaction patterns of tertiary carbenio-phosphines,[17,26] and its course backs thus the operative definition[15] of imidazolio-phosphines as NHC-adducts of elusive phosphenium ions. Despite this analogy, the reactivity of primary and secondary imidazolio-phosphines differs in a qualitative sense from that of their tertiary analogues, as the natural driving force arising from a coupled proton transfer is here unavailable and the reaction needs to be coerced by providing a suitable external energy input.

As a further conclusion, we note that adding an excess of NHC will shift the equilibria of eqns. (7) to (9) to the side of the imidazolio-phosphides. Because parallel trends apply as well to related reactions of oligophosphines (**15-P$_n$**)$^+$, NHCs should make viable reagents for the disassembly of polyphosphine frameworks into imidazolio-phosphides as ultimate fragments. The validity of this forecast has in fact been proven long before in the known syntheses of imidazolio-phosphides from NHCs and cyclic oligophosphines.[6,12] Building on this insight, we can now consider these reactions as reciprocally related to the condensation of imidazolio-phosphines studied in this work: both types of transformations embody in essence a shift of the same coupled equilibria to one side or the other, allowing one to annul the synthesis of imidazolio-phosphides by quenching the NHC with a suitable acid. The reported degradation of an imidazolio-phenylphosphide by triphenylboron[16a] suggests that Lewis-acids may have the same effect.

Dialkylated imidazolio-phosphines.

Imidazolio-monoalkylphosphides **6b** and **8b** react smoothly with alkyl halides or Meerwein salts to afford imidazolio-dialkylphosphines **19**[BF$_4$] (Scheme 9) that are readily isolated as crystalline salts. Depending on the choice of reagent, products with like and different alkyls can be prepared.

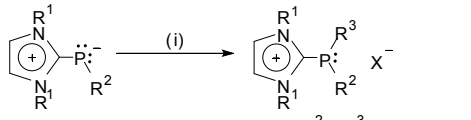

8b (R^2 = Me)
6b (R^2 = Et)

19a[BF$_4$] (R^2 = R^3 = Me)
19b[BF$_4$] (R^2 = R^3 = Et)
19c[X] (R^2 = Me, R^3 = Et, X = I, BF$_4$)

Scheme 9: Alkylation of P-alkyl imidazolio-phosphides.

Crystallographic studies of **19a**[BF$_4$] and **19c**[BF$_4$] reveal that the phosphorus atoms in the cations (Figure 9) exhibit a similar pyramidal coordination and comparable P–C$_{imi}$ and P–C$_{alkyl}$ distances as their secondary congeners (Table 1).

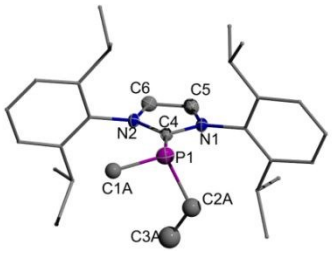

Figure 9. Molecular structure of the cation of **19c[BF$_4$]** in the crystal. For clarity, hydrogen atoms were omitted and N-Dipp substituents drawn using a wire model. Thermal ellipsoids were drawn at the 50% probability level. The P-alkyl substituents are disordered over two positions, only one of which (with occupancy 0.676(4)) is shown. Selected distances are listed in Table 1.

Dimethylated **19a**[I] was also obtained directly from primary imidazolio-phosphide **4b**, by adding first an excess of methyl iodide and then, after monoalkylation to **2b**$^+$ was complete, admitting Hünig's base to produce imidazolio-methylphosphide **8b** that was immediately trapped by leftover alkylating agent. Formation of an appreciable quantity (≈ 25%) of (MeP)$_n$ (n = 3-5) indicates, however, that unwanted condensation of transient **2b**$^+$ is not completely suppressed.

Anticipating that cationic imidazolio-dialkylphosphines display a similar liability towards nucleophilic displacement of the NHC unit as diphenylated derivatives,[17] we explored the reactions of **19a**[BF$_4$] and **19c**[BF$_4$] with LiAlH$_4$. This reagent was chosen because of its ability to serve as a source of both a nucleophilic hydride and an electrophilic aluminium centre for sequestering the released carbene. NMR-spectroscopic analysis of the volatiles collected after distillation confirmed the formation of secondary phosphines (Me_2PH, Me(Et)PH) as main products. The samples contained neither organic by-products traceable to imidazolio-substituents nor boron- or aluminium-containing impurities, thus confirming that the sequestering strategy succeeded, but comprised minor amounts (6-14%) of diphosphines. We envisage that these by-products originate from a dismutation between different phosphorus-containing species or from a SET reaction between a transient NHC and a phosphorus electrophile,[27] but further studies are needed to clarify this issue. Considering that the imidazolio-phosphides used can be produced directly from elemental phosphorus,[8c] their conversion into secondary (di)phosphines marks a new approach to the preparation of simple organophosphorus compounds that bypasses the use of environmentally problematic[1d,e] chlorophosphines.

Conclusions

Primary and secondary imidazolio-phosphines and conjugate imidazolio-phosphides exhibit a diverse chemical behaviour due to their ability to act as Brønsted- as well as Lewis-acids or bases, respectively. The reactivity patterns associated with both modes show both parallels and divergences. Similarities appear in reactions of imidazolio-phosphides with Brønsted-acids or electrophiles to give primary or secondary cationic

phosphines, respectively; divergence is exemplified in the behaviour of the cationic phosphines, which react with Brønsted-bases under attack at the P–H- and with Lewis-bases under attack at the P–C(imidazole) bond. Mutual reactions between imidazolio-phosphines and -phosphides proceed as P–C/P–H σ-bond metatheses under formation of a new P–P bond and release of a P-free imidazolium ion, and can be delineated into an initial nucleophilic (Lewis-type) substitution involving P–P bond formation under liberation of an NHC and an ensuing (Brønsted-type) protonation of the carbene. DFT studies suggest that this last step provides the net driving force for the whole process, and that its kinetic barrier is not caused by a high degree of kinetic inertness of the P–C bonds in the phosphines but rather an unfavourable energy balance of the initial substitution step. The observed reactivity patterns and proposed reaction mechanism back the perception of imidazolio-phosphines as NHC adducts.[15,17,26]

The energetically favourable interplay of nucleophile-induced P–P bond formation and P–H-deprotonation by strong bases enables primary/secondary imidazolio-phosphines to react with a sub-stoichiometric amount of a conjugate phosphide in cascade-like sequences of σ-bond metatheses. Final products are imidazolium salts and imidazole-free polyphosphorus species, and the net reaction qualifies as phosphide-catalysed polycondensation of the cationic phosphines. The reaction cascades embody systems of coupled dynamic equilibria which revert the well-known syntheses of imidazolio-phosphides[6] from NHCs and cyclic oligophosphines. Due to their exergonic nature and low kinetic barriers, these processes compromise the establishing of regular acid/base equilibria between cationic phosphines and their conjugate bases, or between one of these species and an external acid or base. Hence, synthetically useful application of the (de)protonation of imidazolio-phosphines or -phosphides by external bases or acids is only feasible under reaction conditions supressing any direct interaction of both contestants.

Even if the application of phosphorus-heteroatom σ-bond metatheses for the assembly of polyphosphorus frameworks is known,[28] the reactions reported here are to the best of our knowledge the first documented examples involving carbon as heteroatom. Moreover, they provide a rare occasion to obtain insight into the assembly of $(RP)_n$-chains, illustrating a growth mechanism by sequential attachment of P_1-building blocks that involves no free phosphinidenes or phosphenium ions but is best described as a substitution-like process mediated by a nucleophilic catalyst. If one considers that the reported reactions of imidazolio-phosphines relate closely to the dismutation of other (poly)phosphines and the assembly and disassembly of bond networks in elemental phosphorus or polyphosphides,[1b,2] the mechanistic details revealed in this work can improve the understanding of base- or nucleophile-induced growth and disintegration of P–P bonded frameworks in a more general sense, and thus help further advancing a basically important topic in phosphorus chemistry. Recognition of the insight gained may also aid developing new rational pathways to functionalise imidazolio-phosphines.

Conflicts of interest

View Article Online
DOI: 10.1039/D0DT03633A

There are no conflicts to declare.

Acknowledgements

The authors acknowledge financial support by the German Research Foundation (DFG) through grant no. GU 415/17-1. We further thank B. Förtsch for elemental analyses, and J. Trinkner and Dr. W. Frey (both Institute of Organic Chemistry, University of Stuttgart) for the recording of mass spectra and the collection of X-ray data sets, respectively. The computational studies were supported by the state of Baden-Württemberg through bwHPC and the German Research Foundation (DFG) through grant no INST 40/467-1 FUGG (JUSTUS cluster).

Notes and references

‡ A related reaction might have occurred upon treatment of **I-Ph** with BPh_3, but was not investigated further; see ref. 16a.
§ We presume that even smaller quantities are sufficient, although this was not practically tested.
§§ Another, yet undisclosed side-reaction is held responsible for the formation of minor amounts of Et(H)P-P(H)Et (2 diastereomers) as a further transient species.
† Observation of PH_3 as exclusive product is attributable to the known liability of P_2H_4 to react with strong bases under disproportionation, see ref. 2b.

1 a) B. M. Cossairt, N. A. Piro and C. C. Cummins, *Chem. Rev*., 2010, **110**, 4164; b) M. Caporali, L. Gonsalvi, A. Rossin and M. Peruzzini, *Chem. Rev*., 2010, **110**, 4178; c) M. Scheer, G. Balázs and A. Seitz, *Chem. Rev*., 2010, **110**, 4236; d) J. E. Borger, A. W. Ehlers, J. C. Slootweg and K. Lammertsma, *Chem. Eur. J*., 2017, **23**, 11738.
2 a) M. Baudler and K. Glinka, *Chem. Rev*., 1993, **93**, 1623; b) M. Baudler and K. Glinka, *Chem. Rev*., 1994, **94**, 1273.
3 H. G. v. Schnering and W. Hönle, *Chem. Rev*., 1988, **88**, 243.
4 T. Köchner, T. A. Engesser, H. Scherer, D. A. Plattner, A. Steffani and I. Krossing, *Angew. Chem. Int. Ed*., 2012, **51**, 6529.
5 Reviews: a) T. Krachko and J. C. Slootweg, *Eur. J. Inorg. Chem*., 2018, 2734; b) A. Doddi, M. Peters and M. Tamm, *Chem. Rev*., 2019, **119**, 6994.
6 a) A. J. Arduengo, H. V. R. Dias and J. C. A. Calabrese, *Chem. Lett*., 1997, **26**, 143; b) A. J. Arduengo, J. C. Calabrese, A. H. Cowley, H. V. R. Dias, J. R. Goerlich, W. J. Marshall, B. Riegel, *Inorg. Chem*., 1997, **36**, 2151.
7 For an earlier report describing the synthesis of a benzannulated cyanophosphinidene heterocycle without making reference to the carbene-phosphinidene picture see: A. Schmidpeter, W. Gebler, F. Zwaschka, W. S. Sheldrick, *Angew. Chem. Int. Ed. Engl*., 1980, **19**, 722.
8 a) K. Hansen, T. Szilvási, B. Blom, S. Inoue, J. Epping and M. Driess, *J. Am. Chem. Soc*. 2013, **135**, 11795; b) A. M. Tondreau, Z. Benkő, J. R. Harmer and H. Grützmacher, *Chem. Sci*., 2014, **5**, 1545; c) M. Cicač-Hudi, J. Bender, S. H. Schlindwein, M. Bispinghoff, M. Nieger, H. Grützmacher and D. Gudat, *Eur. J. Inorg. Chem*., 2016, 649.
9 For a 4-lithio-derivative, see: Y. Wang, Y. Xie, M. Y. Abraham, R. J. Gilliard, P. Wei, H. F. Schaefer, P. v. R. Schleyer and G. H. Robinson, *Organometallics*, 2010, **29**, 4778.
10 A. Doddi, D. Bockfeld, T. Bannenberg, P. G. Jones, M. Tamm, *Angew. Chem. Int. Ed*., 2014, **53**, 13568.

View Article Online
DOI: 10.1039/D0DT03633A

11 O. Lemp, M. Balmer, K. Reiter, F. Weigend and C. von Hänisch, *Chem. Commun*., 2017, **53**, 7620.
12 T. Krachko, M. Bispinghoff, A. M. Tondreau, D. Stein, M. Baker, A. W. Ehlers, J. C. Slootweg and H. Grützmacher, *Angew. Chem. Int. Ed*., 2017, **56**, 7948.
13 a) L. Weber, B. Quasdorff, H.-G. Stammler and B. Neumann, *Chem. Eur. J*., 1998, **4**, 469; b) L. Weber, U. Lassahn, H.-G. Stammler and B. Neumann, *Eur. J. Inorg. Chem*., 2005, 4590.
14 Z. Kelemen, R. Streubel, L. Nyulászi, *RSC Adv.*, 2015, **5**, 41795.
15 L. Liu, D. A. Ruiz, F. Dahcheh and G. Bertrand, *Chem. Commun*., 2015, **51**, 12732.
16 a) A. J. Arduengo, C. J. Carmalt, J. A. C. Clyburne, A. H. Cowley and R. Pyati, *Chem. Commun*., 1997, 981; b) O. Lemp, C. v. Hänisch, *Phosphorus, Sulfur Silicon Relat. Elem*. 2016, **191**, 659.
17 a) Y. Canac, C. Maaliki, I. Abdellahab and R. Chauvin, *New J. Chem*., 2012, **36**, 17; b) M. Alcarazo, *Acc. Chem. Res*., 2016, **49**, 1797; c) Y. Canac, *Chem. Asian J*., 2018, **13**, 1872.
18 During writing of this manuscript, we became aware of a report on the synthesis of an imidazolio-alkyl-phosphide through a similar approach: J. E. Rodriguez Villanueva, M. A. Wiebe and G. G. Lavoie, *Organometallics*, 2020, **39**, 3260.
19 S. Alvarez, *Dalton Trans*., 2013, **42**, 8617.
20 a) P. Politzer, J. S. Murray and T. Clark, *PCCP*, 2010, **12**, 7748; b) P. Politzer, J. S. Murray, G. V. Janjic and S. D. Zaric, *Crystals*, 2014, **4**, 12; c) P. Politzer, J. S. Murray, T. Clark and G. Resnati, *PCCP*, 2017, **19**, 32166.
21 L. Maier, P. J. Diel and J. C. Tebby, In *CRC Handbook of Phosphorus-31 Nuclear Magnetic Resonance Data*; J. C. Tebby, Ed.; CRC Press: Boca Raton, FL, **1991**; Chapter 6.
22 M. Baudler, J. Hahn and E. Clef, *Z. Naturforsch*., 1984, **39b**, 438.
23 a) D. Dhara, P. Kalita, S. Mondal, R. S. Narayanan, K. R. Mote, V. Huch, M. Zimmer, C. B. Yildiz, D. Scheschkewitz, V. Chandrasekhar and A. Jana, *Chem. Sci*., 2018, **9**, 4235; b) D. Dhara, S. Das, P. Kalita, A. Maiti, S. K. Pati, D. Scheschkewitz, V. Chandrasekhar and A. Jana, *Dalton Trans*., 2020, **49**, 993.
24 a) P. Junkes, M. Baudler, J. Dobbers, D. Rackwitz, *Z. Naturforsch*., 1972, **27b**, 1451.
25 Regarding the analogy between main group elements and transition metals, see: P. P. Power, *Nature*, 2010, **463**, 171.
26 K. Schwedtmann, R. Schoemaker, F. Hennersdorf, A. Bauzá, A. Frontera, R. Weiss and J. J. Weigand, *Dalton Trans*., 2016, **45**, 11384.
27 Z. Dong, C. Pezzato, A. Sienkiewicz, R. Scopelliti, F. Fadaei-Tirani and K. Severin, *Chem. Sci*., 2020, **11**, 7615.
28 a) K.-O. Feldmann and J. J. Weigand, *J. Am. Chem. Soc*. 2012, **134**, 15443; b) R. Schoemaker, K. Schwedtmann, A. Franconetti, A. Frontera, F. Hennersdorf and J. J. Weigand, *Chem. Sci*., 2019, **10**, 11054; c) C. Taube, K. Schwedtmann, M. Noikham, E. Somsook, F. Hennersdorf, R. Wolf and J. J. Weigand, *Angew. Chem. Int. Ed*., 2020, **59**, 3585.

Entry for the Table of Contents

View Article Online
DOI: 10.1039/D0DT03633A

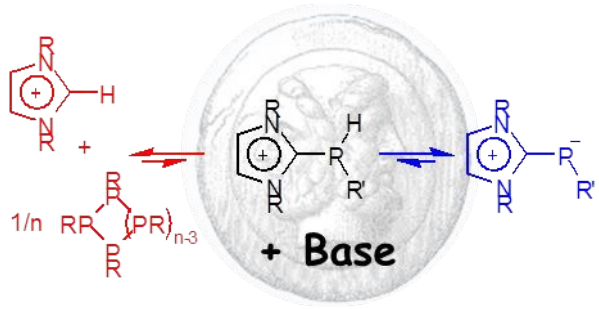

The behaviour of cationic imidazolio-phosphines towards bases is coined by a two-sided reactivity, allowing to access either imidazolio-phosphides via Brønsted-type proton transfers or P-free imidazolium ions and oligophosphines via autocatalytic reaction cascades involving Lewis acid/base-type elementary steps.